PLOS ONE

RESEARCH ARTICLE

Correlating transcription and protein expression profiles of immune biomarkers following lipopolysaccharide exposure in lung epithelial cells

Daniel E. Jacobsen[1], Makaela M. Montoya[1], Trent R. Llewellyn[1], Kaitlyn Martinez[2], Kristen M. Wilding[3], Kiersten D. Lenz[1], Carrie A. Manore[3], Jessica Z. Kubicek-Sutherland[1]*, Harshini Mukundan[1¤]*

1 Chemistry Division, Los Alamos National Laboratory, Los Alamos, New Mexico, United States of America, **2** Analytics, Intelligence and Technology Division, Los Alamos National Laboratory, Los Alamos, New Mexico, United States of America, **3** Theoretical Division, Los Alamos National Laboratory, Los Alamos, New Mexico, United States of America

¤ Current address: Bioscience Area, Lawrence Berkeley National Laboratory, Berkeley, California, United States of America
* jzk@lanl.gov (JZKS); harshini@lanl.gov (HM)

Citation: Jacobsen DE, Montoya MM, Llewellyn TR, Martinez K, Wilding KM, Lenz KD, et al. (2024) Correlating transcription and protein expression profiles of immune biomarkers following lipopolysaccharide exposure in lung epithelial cells. PLoS ONE 19(4): e0293680. https://doi.org/10.1371/journal.pone.0293680

Editor: Sadiq Umar, University of Illinois, UNITED STATES

Received: May 23, 2023

Accepted: October 17, 2023

Published: April 23, 2024

Data Availability Statement: All relevant data can be found on Figshare (https://doi.org/10.6084/m9.figshare.24158991). The python code underlying the analysis can be found on github (https://github.com/dejacobsen15/20230907_lps_paper_code).

Funding: This work was supported by the Defense Threat Reduction Agency (DTRA) to H.M. and C.A. M. The funders had no role in study design, data collection and analysis, decision to publish, or preparation of the manuscript.

Abstract

Universal and early recognition of pathogens occurs through recognition of evolutionarily conserved pathogen associated molecular patterns (PAMPs) by innate immune receptors and the consequent secretion of cytokines and chemokines. The intrinsic complexity of innate immune signaling and associated signal transduction challenges our ability to obtain physiologically relevant, reproducible and accurate data from experimental systems. One of the reasons for the discrepancy in observed data is the choice of measurement strategy. Immune signaling is regulated by the interplay between pathogen-derived molecules with host cells resulting in cellular expression changes. However, these cellular processes are often studied by the independent assessment of either the transcriptome or the proteome. Correlation between transcription and protein analysis is lacking in a variety of studies. In order to methodically evaluate the correlation between transcription and protein expression profiles associated with innate immune signaling, we measured cytokine and chemokine levels following exposure of human cells to the PAMP lipopolysaccharide (LPS) from the Gram-negative pathogen *Pseudomonas aeruginosa*. Expression of 84 messenger RNA (mRNA) transcripts and 69 proteins, including 35 overlapping targets, were measured in human lung epithelial cells. We evaluated 50 biological replicates to determine reproducibility of outcomes. Following pairwise normalization, 16 mRNA transcripts and 6 proteins were significantly upregulated following LPS exposure, while only five (CCL2, CSF3, CXCL5, CXCL8/IL8, and IL6) were upregulated in both transcriptomic and proteomic analysis. This lack of correlation between transcription and protein expression data may contribute to the discrepancy in the immune profiles reported in various studies. The use of multiomic assessments to achieve a systems-level understanding of immune signaling processes can

Competing interests: The authors have declared that no competing interests exist.

result in the identification of host biomarker profiles for a variety of infectious diseases and facilitate countermeasure design and development.

Introduction

The host innate immune response is the body's first line of defense against pathogens [1, 2]. Human innate immune receptors recognize conserved signatures on pathogens known as pathogen associated molecular patterns (PAMPs), which are important signaling molecules released by pathogens during infection [3, 4]. These molecules bind host cell pattern recognition receptors (PRRs) typically found on endothelial, epithelial, or tissue-resident immune cells such as macrophages and dendritic cells triggering a signal cascade that upregulates expression of cytokines and chemokines. For example, Toll-Like-Receptor 4 (TLR4) recognizes lipopolysaccharide (LPS), a PAMP found in Gram-negative bacteria [5]. The activation of TLR4 triggers the nuclear factor κB (NF-κB) pathway and causes the release of cytokines and chemokines [6]. Cytokines and chemokines signal and recruit specific immune cells to the site of infection [7]. Cytokines include a wide array of molecules including interferons (IFNs), interleukins (ILs), colony-stimulating factors (CSFs), tumor necrosis factors (TNFs), and transforming growth factors (TGFs) [8]. Chemokines are divided into groups by the positioning of their initial cysteine residues: XC, CC, CXC, and CX3C. CC chemokine ligands (CCLs) have two adjoining cysteine residues, CXC ligands (CXCLs) have an amino acid between the cysteine residues [9]. Neutrophils are among the first responders, stimulate leukocyte signaling, phagocytosis, and degranulation [10]. Monocytes differentiate into either macrophages for phagocytosis of extracellular pathogens or dendritic cells (DCs) for antigen presentation [11].

Cultured human cell studies are often used as a model for generating biological insights about specific aspects of a given disease [12]. Cell systems do not entirely replicate the physiological complexity of innate immune recognition, but they provide a reliable and effective model for controlled studies, including the ability to expose cells to individual pathogens or molecules and measure responses over time. However, most cell studies are limited in scope by focusing on a few key cytokine and chemokine targets and avoiding biological variation by using a small number of replicates [13, 14]. Typically, these studies are designed to measure either transcription (mRNA) or protein responses, not both, resulting in limited data sets allowing for a direct comparison of potential mRNA and protein biomarkers of host responses to specific stimuli [15, 16]. Cell regulation is determined by the interplay between mRNA, protein, metabolites and other components of the regulome [17]. Recent studies have highlighted the poor correlation between mRNA and protein profiles in the same experimental system, highlighting the role of other factors such as post-transcriptional machinery in modulating cellular responses [18–21]. In order to begin to explore the correlation between transcriptomic and proteomic profiles in innate immunity, we present a methodical comparison of transcription and protein immune profiles in lung epithelial cells exposed to LPS derived from *Pseudomonas aeruginosa*, a common model for lung response to infection by Gram-negative bacteria [22]. We examined expression of 84 mRNA transcripts and 69 secreted proteins, including 35 overlapping targets, from 5 biological replicates. Supernatants for protein measurements and cell extracts for mRNA measurements were taken at the same time from the same cells, providing a paired examination of mRNA and protein levels. This is a first step towards developing a multiomic approach to understanding innate immune signaling and identifying host biomarker profiles to diagnose and detect infectious diseases.

Materials and methods

Cell culture and LPS exposure

Human lung epithelial A549 cells were obtained from American Type Culture Connection (ATCC; CCL-185) and cultured in Kaighn's Modified Ham's Formulation F-12 Media (ThermoFisher Scientific; 21127022) with 10% fetal bovine serum (Sigma Aldrich; F2442-500ML) and 1% v/v penicillin/streptomycin (ThermoFisher Scientific; 15140122). Two stocks (frozen at passage #4) were grown separately for a single passage, then split into 6 separate cultures each (total of 12). These 12 flasks, referred to as lineages, were grown for an additional passage to increase biological variation. Over the course of 3 weeks, 5 passages of each cell line were cultured in 24-well plates, with each of the 12 lineages cultured in 2 wells. The night before adding to cells, LPS from *P. aeruginosa* suspended in water (Sigma Aldrich; L9143-25MG) was sonicated and diluted to 10 μg/mL in fresh media and stored overnight at 4˚C. Once cells reached >80% confluence, the media in one well of each lineage was replaced with media pre-warmed to 37˚C containing 10 μg/mL LPS (treated), while the other well received fresh, pre-warmed media without LPS (untreated). After 24 hours, the supernatant was removed and stored at –80˚C until protein analysis and RNA was extracted from the cells using the Qiagen RNeasy Mini Kit (Qiagen; 74106). Post-extraction, RNA concentration was measured using the Qubit RNA Broad Range Assay Kit (ThermoFisher Scientific; Q10211) and stored at –80˚C until further use.

Transcript expression analysis

500 ng RNA from each sample was used as input for first strand synthesis (Qiagen; 330404). After first strand synthesis, samples were run on 96-well Human Cytokines and Chemokines RT2 Profiler PCR Arrays (Qiagen; PAHS-150ZC-24) using the RT2 qPCR Master Mix (Qiagen; 330529). The Cytokine and Chemokine RT2 array measured RNA levels of 84 cytokines and chemokines, 5 housekeeping genes, and included 7 control wells. mRNA expression was measured for 100 replicates, 50 LPS-treated and 50 matching untreated controls from the same lineage and plate. The plates were run on an Applied Biosystems StepOnePlus Real-Time PCR Thermocycler (ThermoFisher Scientific; 4376600) using the following protocol: 95˚C for 10 min; 40 cycles: 95˚C for 15 sec; 60˚C for 1 min. Cycle threshold (C_T) values were used as input for data analysis and normalized to the housekeeping gene beta-2 microglobulin (B2M). B2M was chosen as the housekeeping gene due to it having the least-significant difference between treated and untreated samples (see S1 Fig). Fold change, also commonly termed relative quantification or RQ, was calculated using pairwise $2^{-\Delta\Delta CT}$ for each transcript target *T*, which is the difference in normalized C_T between the LPS-treated sample (+) and its untreated control (-) from the same lineage *l* and plate *p*, then averaged across all *N* samples,

$$Fold\ Change_T = \frac{\sum_{p,l} 2^{-\Delta\Delta CT_{T,\,p,\,l}}}{N} \tag{1}$$

$$2^{-\Delta\Delta CT_{T,\,p,\,l}} = 2^{-\left(\Delta CT_{T,p,l,+} - \Delta CT_{T,p,l,-}\right)} \tag{2}$$

$$\Delta CT_{T,p,l,t} = CT_{T,p,l,t} - CT_{B2M,p,l,t} \text{ for } t = +, - \tag{3}$$

Protein analysis

Supernatants were analyzed for secreted proteins using the abcam FirePlex Discovery Human Cytokine and Chemokine panel (abcam; ab243551), which measures protein levels of 69 cytokines and chemokines and a negative control used for normalization. 35 of the proteins measured had their corresponding mRNA measured in transcript analysis above, providing direct comparison between mRNA and protein levels. Prior to starting the FirePlex protocol, supernatants were centrifuged at 2000 x g for 15 minutes to remove debris. Samples were processed using the vacuum filtration plate option of the FirePlex protocol, vacuum filtration manifold (abcam; ab204067), and analyzed on a Beckman Coulter CytoFLEX S Flow Cytometer (Beckman Coulter; C09766). The cytometer measured FITC (gain 70), PE (gain 50), and PC5.5 (gain 15), using a flow rate of 60 μL/min with samples run for 3 minutes or 5,000 events of FITC signal ≥10,000. Raw output from the flow cytometer was analyzed using the Firefly Analysis Workbench software from abcam (https://www.fireflybio.com), which generated measurements of signal for each sample and protein. Known standards for each protein were also run in the FirePlex assay and used to convert signal measurements to concentrations in pg/mL. For comparative analysis, values above the maximum signal of the standard curve were capped at the maximum value and values below the minimum signal of the standard curve were capped at the minimum. Normalized protein concentrations $[\bar{P}]$ were obtained by dividing each pg/mL value $[P]$ by the control ratio value CR, which was the value of the negative control $[NC]$ for that sample divided by the average negative control value across all samples. Fold-change for each protein target T was calculated by pairwise division of normalized pg/mL treated values by untreated values, then pairwise-calculated fold-change was averaged across plates p and lineages l.

$$Fold\ Change_{\ T} = \frac{\sum_{p,l} \frac{[\bar{P}]_{T,p,\ l,+}}{[\bar{P}]_{T,p,\ l,-}}}{N} \tag{4}$$

$$[\bar{P}]_{T,p,l,t} = \frac{[P]_{T,p,l,t}}{CR_{p,l,t}} \text{ for } t = +, - \tag{5}$$

$$CR_{p,\ l,t} = \frac{[NC]_{p,\ l,t}}{\frac{\sum_{p,\ l,t} [NC]_{p,\ l,t}}{N}} \text{ for } t = +, - \tag{6}$$

Some protein samples detected no particles, meaning no FirePlex particles for a protein were detected by the flow cytometer for that individual sample. As this non-detection does not indicate absence of the protein in the sample but is the result of dropouts from random sampling, these data cannot be considered true zeros. As a result, these samples were left out of the analysis, as well as the analogous treated/untreated sample from the same lineage and plate for pairwise comparisons.

Statistical analysis

Statistical analyses were performed using python 3.8.8 [23]. Significance of mRNA expression was determined by pairwise Student's t-test between B2M-normalized C_T values ($\Delta CT_{T,p,l,t}$ values in Eq 3 above) of LPS-treated samples and their corresponding untreated control. Significance in protein expression was calculated by pairwise Student's t-test between LPS-treated samples and their corresponding untreated control using data normalized with negative control of each sample and converted to pg/mL. These values were chosen so that a pairwise

Student's t-test could be used, reflecting the paired treated/untreated sample of each plate and lineage.

Results and discussion

Generation of reproducible transcription and protein expression profiles following LPS exposure in lung epithelial cells

Human lung epithelial A549 cells were selected for this study. A549 cells are not a comprehensive model for lung infection but have been used often for simple controlled studies of LPS stress on cells [14, 24, 25]. Biological replicates of A549 cells in this study were derived from twelve lineages, produced from two frozen stocks at the same passage number, then split into six new flasks each and harvested at five time points (Fig 1a). At the five time points, cells were

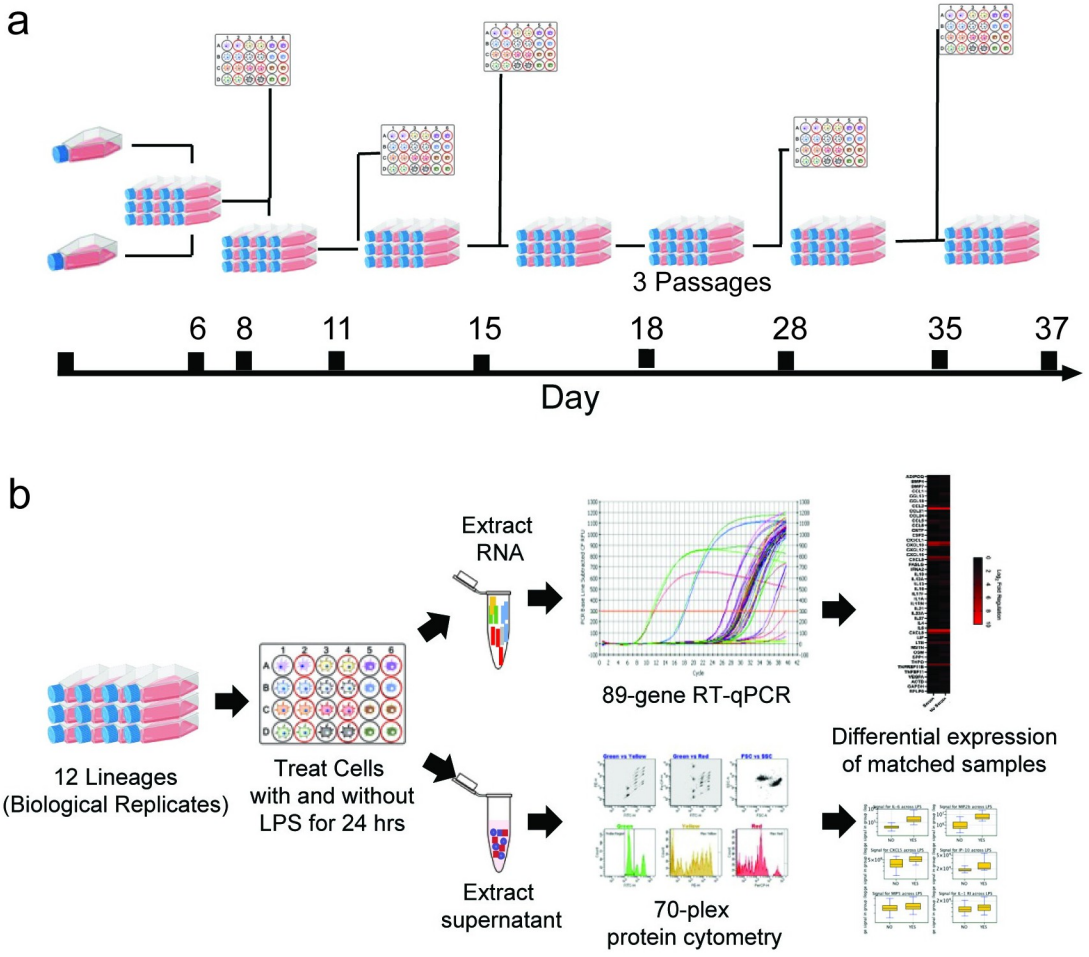

Fig 1. Schematic of experimental workflow evaluating mRNA and protein expression of lung epithelial cells following LPS exposure. a) Timeline of experiments. Two cell stocks at the same passage number were thawed and cultured. After one passage, stocks were split into six flasks each (12 total lineages). At five timepoints over 11 passages, samples were collected from each lineage. b) At each of the five time points, each lineage was seeded in two wells of a 24-well plate. One well was treated with 10 μg/mL LPS diluted in media, the other received fresh media without LPS (untreated), and all were incubated for 24 hours at 37˚C with 5% CO_2 prior to harvesting of mRNA and supernatant. mRNA levels were evaluated using reverse-transcription quantitative polymerase chain reaction (RT-qPCR) and protein levels were measured in supernatants using immunoassays. Figure created with BioRender.com.

https://doi.org/10.1371/journal.pone.0293680.g001

seeded in 24-well plates, with each of the twelve lineages receiving two wells (Fig 1b). Near confluency, one of the wells of each lineage received media containing 10 μg/mL LPS (treated), and the other well received fresh media (untreated), and then both were incubated for 24 hours prior to harvesting. 10 μg/mL LPS was found to be enough to stimulate an immune response without reducing cell viability (S2 Fig and [24]). Incubation of 24 hours was chosen to provide more consistent results, as dynamic changes in protein levels make the early time-points more variable [26]. For harvesting, supernatant of each sample was used for protein analysis and the cells were harvested for mRNA analysis (see S1 Methods in S1 File). Each biological replicate had two wells used for treated and untreated controls, so pairwise analysis was used to compare LPS-treated expression profiles relative to the matched untreated control prior to averaging across all samples. This was necessary to reduce bias caused by lineage and plate (S3 Fig). In this study, 50 biological replicates with matched treated and untreated controls were analyzed for mRNA and protein expression to identify biomarkers of LPS exposure.

Biomarkers of LPS exposure in lung epithelial cells include cytokines and chemokines involved in cellular recruitment and pro-inflammatory responses

Expression levels of human cytokines and chemokines were evaluated using commercial kits including 84 mRNA and 69 protein targets. In response to LPS treatment, 16 cytokines and chemokines showed significant upregulation in mRNA expression (Fig 2a). Four of them (CXCL1, CXCL2, CXCL5, and CXCL8) are chemokines involved in neutrophil recruitment [27]. Seven of them (CCL2, CCL5, CCL17, CCL20, CCL22, CXCL10, and IL7) are involved in monocyte and T cell recruitment [28–34]. T cells are recruited to early sites of inflammation including $CD4^+$ T helper (T_H) cells that produce cytokines to orchestrate coordinated immune responses [35]. Different cell subsets target different types of pathogens, with T_H1 cells targeting intracellular viruses and bacteria, T_H2 cells targeting extracellular parasites, and T_H17 cells targeting extracellular bacteria. Naïve $CD4^+$ T cells may also divide into regulatory T cells (T_{reg}) that suppress immune responses. CCL17 and CCL22 have high selectivity towards T_H2 cells [36], which are known to be promoted in response to LPS [37]. CCL20 is primarily involved in recruitment of T_H17 effector T cells. CXCL10 primarily affects T_H1 effector T cells

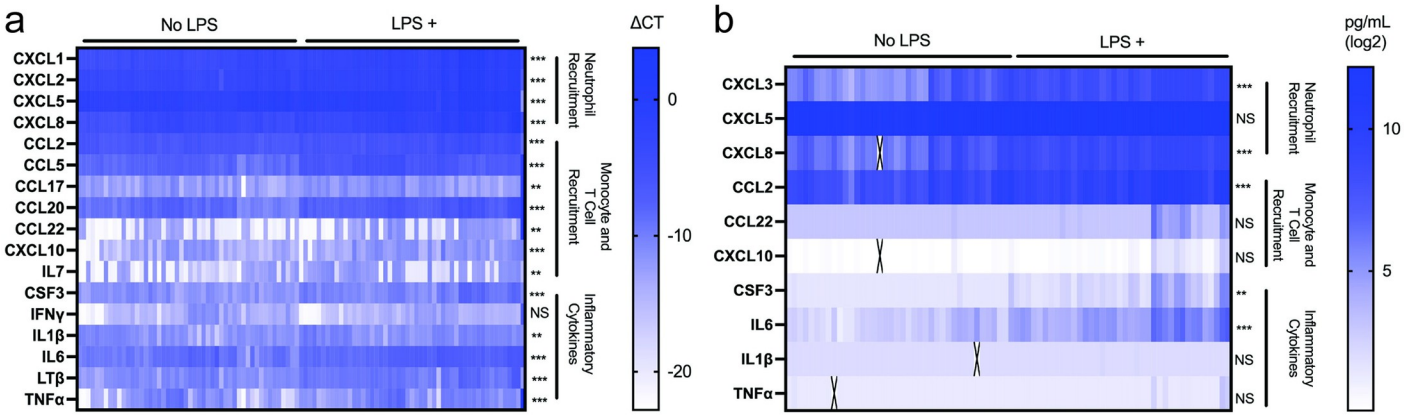

Fig 2. mRNA and protein expression profiles in response to LPS exposure. Each column represents an individual biological replicate for (a) mRNA and (b) protein analysis. mRNA values are displayed as ΔC_T values following normalization to the housekeeping gene B2M C_T value (see S1 Methods in S1 File). Protein values are displayed as log2 pg/mL following normalization to negative control (see S1 Methods in S1 File). Student's paired t-tests were performed comparing LPS-treated to untreated samples of the same plate and lineage (***$p<0.001$; **$p<0.01$; NS, not significant). IL, interleukin; CCL, chemokine ligand; CXCL, chemokine (C-X-C motif) ligand; TNFα, tumor necrosis factor alpha; IFNγ, interferon gamma; LTβ, lymphotoxin beta; CSF, colony stimulating factor.

https://doi.org/10.1371/journal.pone.0293680.g002

and has been more closely associated with viral infections [38]. CCL2 has been shown to have a significant effect on monocytes, inducing chemotaxis, differentiation into macrophages, and adhesion to endothelium.

Five pro-inflammatory cytokines (CSF3, IL1β, IL6, lymphotoxin β (LTβ), and TNFα) were also significantly upregulated. CSF3 is a potent stimulator of myeloid cell proliferation and preferentially directs myeloid progenitors into neutrophil differentiation [39]. LTβ signaling is associated with tertiary development of lymphoid tissue [40] and has been linked with neutrophil inflammation [41]. IL6, TNFα, and IL1β are cytokines with systemic, wide-ranging effects, and increased expression following LPS exposure has been shown previously [14]. Additionally, increased levels of these cytokines have been associated with increased severity of respiratory distress [42].

Protein expression showed only six significantly upregulated proteins (Fig 2b). CXCL5 signal was saturated in the FirePlex assay, but enzyme-linked immunosorbent assay (ELISA) results showed a significant increase from LPS treatment (See S1 Methods and S4 Fig). Five of the six significantly upregulated proteins (CCL2, CSF3, CXCL5, CXCL8, and IL6) were upregulated in both mRNA and protein levels. The other protein, CXCL3 [43], is involved in neutrophil recruitment. CXCL3 is part of a subset of chemokines known as Growth Related Oncogene (GRO) chemokines, along with CXCL1 and CXCL2. In this study, CXCL1 and CXCL2 were only investigated in mRNA while CXCL3 was only investigated in protein due to the composition of the commercial panels used. All three were significantly upregulated indicating the neutrophil recruitment pathway as a potential biomarker for LPS exposure at both the transcript and protein expression levels.

Differences in cytokine and chemokine mRNA and protein expression profiles can be used as biomarkers for LPS exposure

Of the 84 mRNA and 69 protein targets, 35 overlapped and were evaluated in both data sets for differences in fold-change (Fig 3a) and significance (Fig 3b). Five cytokines and chemokines were significantly upregulated in both mRNA and protein: CCL2 (Fig 3c), CSF3 (Fig 3d), CXCL5 (Fig 3e), CXCL8/IL8 (Fig 3f), and IL6 (Fig 3g). For all five cytokines and chemokines, the average fold-change of mRNA and protein was identical. These cytokines and chemokines promote neutrophil differentiation (CSF3) and recruitment (CXCL5 and CXCL8), monocyte recruitment (CCL2), and general inflammation (IL6). All five can be used as biomarkers for LPS exposure at both the transcript and protein level.

Four cytokines and chemokines were significantly upregulated in mRNA measurements, but not in protein (IL1β, TNFα, CXCL10, and CCL22). All four have regulatory mechanisms with additional checkpoints between mRNA expression and mature protein secretion. Two cytokines with mRNA and protein discrepancies, IL1β and TNFα, are two of the most potent immune stimulators with systemic effects [44, 45]. As a result, both proteins have several checkpoints before secretion. LPS-binding to TLR4 can initiate IL1β transcription and translation into a pro-IL1β form that remains in the cytosol [46]. The cleavage of pro-IL1β into its secreted form is dependent on the inflammasome signaling pathway [47]. Previous studies indicate that LPS at 10 μg/mL, the concentration used in this study, does not induce inflammasome signaling [24], supporting the absence of IL1β protein upregulation in our experiments. TNFα is produced in an inert, trimeric form that resides on the cellular membrane. This form is cleaved by a disintegrin and metalloprotease 17 (ADAM17; also known as TNFα converting enzyme, TACE) [48]. Previous work in gastric epithelial cells showed that ADAM17 cleavage of membrane-bound TNFα can be induced by Epidermal Growth Factor Receptor (EGFR) activation by *Helicobacter pylori* or by

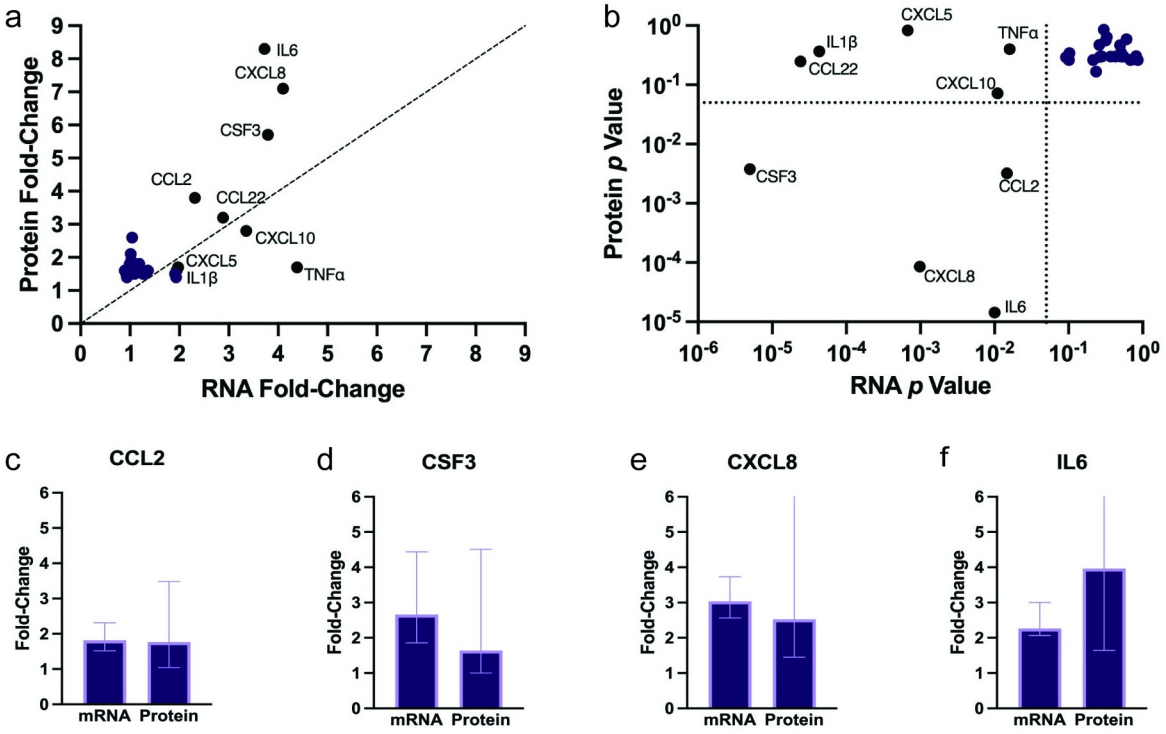

Fig 3. LPS exposure results in discrepancies in mRNA and protein expression profiles of key cytokines and chemokines. (a) Fold-changes in mRNA (x-axis) versus protein (y-axis) expression comparing LPS-treated to untreated controls. Dashed line indicates equivalent RNA and protein fold-changes. (b) *p*-values from pairwise Student's t-test for RNA (x-axis) versus protein (y-axis) fold-changes. Dashed lines indicate $p = 0.05$. Cytokines and chemokines without significant changes in expression of mRNA and/or protein were not displayed. Significance was calculated using paired Student's t-test comparing LPS-treated cells to untreated controls from the same lineage and plate. Individual plots comparing fold-changes in cytokines and chemokines significantly upregulated in both mRNA and protein expression for (c) CCL2, (d) CSF3, (e) CXCL5, (f) CXCL8, and (g) IL6. Values represent median signal and bars represent 95% confidence interval. Significance was calculated using pairwise-Student's t-test matching mRNA and protein fold changes from the same lineage and plate. CXCL5 values represent values obtained via ELISA data (see S1 Methods and S4 Fig). No significant difference was found between mRNA and protein levels. IL, interleukin; CCL, chemokine ligand; CXCL, chemokine (C-X-C motif) ligand; TNF, tumor necrosis factor alpha; CX3CL, (C-X3-C) chemokine ligand; CSF, colony stimulating factor.

https://doi.org/10.1371/journal.pone.0293680.g003

exogenous TNFα [49]. Another study found that intestinal epithelial cells do not produce TNFα following LPS exposure, however gut macrophages release TNFα and stimulate secretion [50].

The chemokine CXCL10 has been shown to require signals from TH_1 effector T cells for secretion by epithelial cells [51]. CCL22 secretion by intestinal epithelial cells has been shown to be stimulated by TNFα [52] and has been shown to promote recruitment of TH_2 cells [53] and T_{reg} cells [54] when secreted by immune cells.

To confirm that the four proteins were not upregulated from LPS treatment, ELISA was performed for these genes and CXCL8 as a positive control in both cell supernatant and cell extract (S4 Fig). ELISA was also performed on CXCL5 using diluted samples, since CXCL5 had saturated signal in the FirePlex assay. Supernatants were used for proteomic analysis because cytokines and chemokines are signaling molecules that must typically be secreted to have an effect. However, intracellular protein levels may provide additional information of cytokines and chemokines not yet secreted or that have been taken up by cells, and so they were examined by ELISA as well. The ELISA results confirmed four proteins were not upregulated in supernatant or cell extract. ELISA analysis of intracellular and extracellular protein

levels on six selected genes also suggested that intracellular protein behavior in response to LPS mirrored that of secreted protein behavior.

There is a significant discrepancy between mRNA and protein profiles of cytokines and chemokines at a single time point, as evidenced by our findings. As described above, additional regulation mechanisms may prevent increased mRNA levels from translating to increased secreted protein levels for the five genes with discrepancies in this study. These discrepancies can shed light into mechanisms of LPS action in different cell systems. In particular, the four genes noted above have been shown to be secreted following signaling by immune cells. For biomarker discovery, this indicates that mRNA expression may be more sensitive to pathogens, as protein regulation has additional checkpoints before secretion. This indicates mRNA analysis in early infection can yield a more comprehensive expression profile supporting disease-specific diagnostics.

Conclusion

Immune responses are a complex interaction of many cell types. Identifying host biomarkers of PAMP or pathogen exposure can be difficult due to this complexity. In this work, we developed a large-scale experimental protocol with 50 biological replicates to investigate the reproducibility of resolution phase immune responses from human lung epithelial cells in response to LPS exposure. We compared expression profiles of cytokines and chemokines for 84 mRNA transcripts and 69 secreted proteins, with 35 overlapping. We found that LPS exposure results in the statistically significant upregulation of 16 mRNA transcripts and only 6 proteins. Furthermore, our work demonstrated four examples of genes whose mRNA expression was significantly upregulated without a corresponding increase in protein. This finding highlights the caution that works should use in assuming that protein upregulation matches mRNA expression upregulation and vice versa. Multiomics approaches can address this problem, as can single omics experiments that focus on biomarkers specific to that omics. In this experiment, we found that transcription analysis provided the more promising means for identifying a unique expression profile for *P. aeruginosa* LPS exposure in lung epithelial cells. Future work will determine the feasibility of using human cytokine and chemokine expression levels to distinguish exposure to different PAMPs or pathogens as a means for diagnosing any infection. The complexity of these responses is not readily amenable to manual decoding. Machine learning algorithms can be a powerful tool to analyze these types of datasets and identify immune response expression profiles associated with specific PAMPs or pathogen infections [2, 55, 56].

Supporting information

S1 Fig. Evaluation of mRNA expression of housekeeping genes. Housekeeping genes C_T values across all samples for LPS+ and LPS- samples. Effect of LPS treatment (mean difference) and its corresponding p-value were determined for each housekeeping gene. B2M showed the smallest effect size from LPS (mean difference = -0.0897) and largest p-value (p-value = 0.552), indicating it as the best gene to use for normalization.
(TIF)

S2 Fig. Cell viability across LPS concentrations. Cell viability, measured as the increase in NucBlue ReadyProbe stain (Hoechst 33342) over a 24-hour period for cells incubated with varying concentrations of LPS. All samples are normalized to the increase seen in cells incubated with no LPS. Error bars represent standard deviation of 3 bioreplicates, which were each determined as the average of 4 technical replicates (4 different wells on a 96 well plate). Line

represents best fit using log-scale concentration.
(TIF)

S3 Fig. Paired normalization of samples reduces bias caused by date of experiment. Principal component analysis (PCA) of mRNA expression data. (a) Percentage of variance explained by each principal component in mRNA expression data normalized by that sample's B2M housekeeping gene expression. (b) Pearson r correlation of each principal component of normalized mRNA data with three main variables of experiment, LPS treatment, date of experiment (Plate), and lineage. Principal component (PC) 1 correlates most closely with plate (Pearson r = 0.54) while PC 2 correlates most closely with LPS treatment (Pearson r = 0.61). (c-f) Each dot represents principal component values of (c, d) expression data normalized to that sample's B2M housekeeping gene expression, (e, f) or pairwise-normalized data of one treated/untreated pair for a given lineage and date. (c) PC 1 and PC 2 of normalized expression data, with colors/numbers indicating date of experiment, with "1" being the first date and "5" being the last date. (d) PC 1 and PC 2 of normalized expression data, with colors indicating LPS treatment of sample. Pairwise-normalized data does not correlate well in PC 1 (13.6% of variance) or PC 2 (11.2% of variance) with either (e) experiment date or (f) lineage. (g) Percentage of variance explained by each principal component in protein data normalized by that sample's negative control (see S1 Methods in S1 File). (h) Pearson r correlation of each principal component of normalized protein expression data with three main variables of experiment, LPS treatment, date of experiment (Plate), and lineage. PC 5 is the first principal component for which LPS treatment is the strongest correlated category.
(TIF)

S4 Fig. ELISA measurements of supernatant and cell extracts. Measured concentrations in pg/mL from matching cell supernatant and cell extract for LPS-treated and untreated A549 cells. Error bars represent standard deviations of 4 biological replicates for supernatants (circles) or cell extracts (triangles). Biological replicate values are the average of three technical replicates, separate wells of a 24-well plate cultured with cells from the same source flask. Student's paired t-test was performed comparing biological replicates of LPS-treated and untreated samples ($^{*}p<0.05$; $^{***}p<0.001$). IL, interleukin; CCL, chemokine ligand; CXCL, chemokine (C-X-C motif) ligand; TNF, tumor necrosis factor alpha.
(TIF)

S1 Methods. Supplemental methods. Explanation of methods used in generating supplemental figures.
(DOCX)

Acknowledgments

This work was performed at the Los Alamos National Laboratory, operated by Triad National Security LLC, for the National Nuclear Security Administration of the United States Department of Energy (Contract No. 89233218CNA000001). The authors thank Dr. Sweta Batni, program manager at DTRA, for her support of this work. The views expressed in this article are those of the authors and do not reflect the official policy or position of the U.S. Department of Defense or the U.S. Government.

Author Contributions

Conceptualization: Carrie A. Manore, Jessica Z. Kubicek-Sutherland, Harshini Mukundan.

Formal analysis: Daniel E. Jacobsen, Makaela M. Montoya, Trent R. Llewellyn, Kaitlyn Martinez, Kristen M. Wilding, Kiersten D. Lenz, Jessica Z. Kubicek-Sutherland.

Funding acquisition: Carrie A. Manore, Harshini Mukundan.

Investigation: Daniel E. Jacobsen, Makaela M. Montoya, Trent R. Llewellyn, Kaitlyn Martinez, Kristen M. Wilding, Kiersten D. Lenz, Carrie A. Manore, Jessica Z. Kubicek-Sutherland, Harshini Mukundan.

Methodology: Daniel E. Jacobsen, Makaela M. Montoya, Trent R. Llewellyn, Kaitlyn Martinez, Kristen M. Wilding, Kiersten D. Lenz, Carrie A. Manore, Jessica Z. Kubicek-Sutherland, Harshini Mukundan.

Project administration: Carrie A. Manore, Harshini Mukundan.

Resources: Carrie A. Manore, Jessica Z. Kubicek-Sutherland, Harshini Mukundan.

Supervision: Carrie A. Manore, Jessica Z. Kubicek-Sutherland, Harshini Mukundan.

Validation: Daniel E. Jacobsen, Makaela M. Montoya.

Visualization: Daniel E. Jacobsen, Jessica Z. Kubicek-Sutherland.

Writing – original draft: Daniel E. Jacobsen, Jessica Z. Kubicek-Sutherland.

Writing – review & editing: Daniel E. Jacobsen, Makaela M. Montoya, Trent R. Llewellyn, Kaitlyn Martinez, Kristen M. Wilding, Kiersten D. Lenz, Carrie A. Manore, Jessica Z. Kubicek-Sutherland, Harshini Mukundan.

References

1. Niimi K, Morimoto M. Cytokine elevation in the mouse small intestine at the early stage of infection with the gastrointestinal parasite Heligmosomoides polygyrus. J Vet Med Sci. 2021; 83(4):573–80. Epub 20210217. https://doi.org/10.1292/jvms.20-0498 PMID: 33597317.
2. Zhang J, Friberg IM, Kift-Morgan A, Parekh G, Morgan MP, Liuzzi AR, et al. Machine-learning algorithms define pathogen-specific local immune fingerprints in peritoneal dialysis patients with bacterial infections. Kidney Int. 2017; 92(1):179–91. Epub 20170317. https://doi.org/10.1016/j.kint.2017.01.017 PMID: 28318629.
3. Takeuchi O, Akira S. Pattern Recognition Receptors and Inflammation. Cell. 2010; 140(6):805–20. https://doi.org/10.1016/j.cell.2010.01.022 PMID: 20303872
4. Roh JS, Sohn DH. Damage-Associated Molecular Patterns in Inflammatory Diseases. Immune Netw. 2018; 18(4):e27. Epub 20180813. https://doi.org/10.4110/in.2018.18.e27 PMID: 30181915.
5. Ciesielska A, Matyjek M, Kwiatkowska K. TLR4 and CD14 trafficking and its influence on LPS-induced pro-inflammatory signaling. Cellular and Molecular Life Sciences. 2021; 78(4):1233–61. https://doi.org/10.1007/s00018-020-03656-y PMID: 33057840
6. Verstrepen L, Bekaert T, Chau TL, Tavernier J, Chariot A, Beyaert R. TLR-4, IL-1R and TNF-R signaling to NF-kappaB: variations on a common theme. Cell Mol Life Sci. 2008; 65(19):2964–78. https://doi.org/10.1007/s00018-008-8064-8 PMID: 18535784.
7. Borish LC, Steinke JW. 2. Cytokines and chemokines. Journal of Allergy and Clinical Immunology. 2003; 111(2, Supplement 2):S460–S75. https://doi.org/10.1067/mai.2003.108 PMID: 12592293
8. Liu C, Chu D, Kalantar-Zadeh K, George J, Young HA, Liu G. Cytokines: From Clinical Significance to Quantification. Adv Sci (Weinh). 2021; 8(15):e2004433. Epub 20210610. https://doi.org/10.1002/advs.202004433 PMID: 34114369.
9. Sokol CL, Luster AD. The chemokine system in innate immunity. Cold Spring Harb Perspect Biol. 2015; 7(5). Epub 20150129. https://doi.org/10.1101/cshperspect.a016303 PMID: 25635046.
10. Chan L, Karimi N, Morovati S, Alizadeh K, Kakish JE, Vanderkamp S, et al. The Roles of Neutrophils in Cytokine Storms. Viruses. 2021; 13(11):2318. https://doi.org/10.3390/v13112318 PMID: 34835125
11. Coillard A, Segura E. In vivo Differentiation of Human Monocytes. Front Immunol. 2019; 10:1907. Epub 20190813. https://doi.org/10.3389/fimmu.2019.01907 PMID: 31456804.

12. Sender V, Stamme C. Lung cell-specific modulation of LPS-induced TLR4 receptor and adaptor localization. Commun Integr Biol. 2014; 7:e29053. Epub 20140516. https://doi.org/10.4161/cib.29053 PMID: 25136402.

13. Li S, Zhao L, Li X, Shang G, Gao L, Song Z, et al. Mir-204 Regulates LPS-Induced A549 Cell Damage by Targeting FOXK2. J Healthc Eng. 2021; 2021:7404671. Epub 20211130. https://doi.org/10.1155/2021/7404671 PMID: 34900201.

14. Sul OJ, Ra SW. Quercetin Prevents LPS-Induced Oxidative Stress and Inflammation by Modulating NOX2/ROS/NF-kB in Lung Epithelial Cells. Molecules. 2021; 26(22). Epub 20211117. https://doi.org/10.3390/molecules26226949 PMID: 34834040.

15. Pal R, Schaubhut J, Clark D, Brown L, Stewart JJ. Single-Cell Analysis of Cytokine mRNA and Protein Expression by Flow Cytometry. Current Protocols in Cytometry. 2020; 92(1):e69. https://doi.org/10.1002/cpcy.69 PMID: 32092227

16. Jiang L, Wang M, Lin S, Jian R, Li X, Chan J, et al. A Quantitative Proteome Map of the Human Body. Cell. 2020; 183(1):269–83.e19. Epub 20200910. https://doi.org/10.1016/j.cell.2020.08.036 PMID: 32916130.

17. Buccitelli C, Selbach M. mRNAs, proteins and the emerging principles of gene expression control. Nature Reviews Genetics. 2020; 21(10):630–44. https://doi.org/10.1038/s41576-020-0258-4 PMID: 32709985

18. Jovanovic M, Rooney MS, Mertins P, Przybylski D, Chevrier N, Satija R, et al. Dynamic profiling of the protein life cycle in response to pathogens. Science. 2015; 347(6226):1259038. https://doi.org/10.1126/science.1259038 PMID: 25745177

19. Harnik Y, Buchauer L, Ben-Moshe S, Averbukh I, Levin Y, Savidor A, et al. Spatial discordances between mRNAs and proteins in the intestinal epithelium. Nature Metabolism. 2021; 3(12):1680–93. https://doi.org/10.1038/s42255-021-00504-6 PMID: 34931081

20. Liu Y, Beyer A, Aebersold R. On the Dependency of Cellular Protein Levels on mRNA Abundance. Cell. 2016; 165(3):535–50. https://doi.org/10.1016/j.cell.2016.03.014 PMID: 27104977

21. Fortelny N, Overall CM, Pavlidis P, Freue GVC. Can we predict protein from mRNA levels? Nature. 2017; 547(7664):E19–E20. https://doi.org/10.1038/nature22293 PMID: 28748932

22. Xu B, Wang H, Chen Z. Puerarin Inhibits Ferroptosis and Inflammation of Lung Injury Caused by Sepsis in LPS Induced Lung Epithelial Cells. Frontiers in Pediatrics. 2021; 9. https://doi.org/10.3389/fped.2021.706327 PMID: 34422728

23. Van Rossum G, and Drake, F.L. Python 3 Reference Manual. Scotts Valley, CA2009.

24. Nova Z, Skovierova H, Strnadel J, Halasova E, Calkovska A. Short-Term versus Long-Term Culture of A549 Cells for Evaluating the Effects of Lipopolysaccharide on Oxidative Stress, Surfactant Proteins and Cathelicidin LL-37. Int J Mol Sci. 2020; 21(3). Epub 20200209. https://doi.org/10.3390/ijms21031148 PMID: 32050475.

25. Xu Q, Huang GD, Duan GC, Qin HJ. MicroRNA-147b alleviates inflammation and apoptosis in acute lung injury via inhibition of p38 MAPK signaling pathway. Eur Rev Med Pharmacol Sci. 2021; 25(4):1974–81. https://doi.org/10.26355/eurrev_202102_25098 PMID: 33660808.

26. Stromberg LR, Mendez HM, Kubicek-Sutherland JZ, Graves SW, Hengartner NW, Mukundan H. Presentation matters: Impact of association of amphiphilic LPS with serum carrier proteins on innate immune signaling. PLOS ONE. 2018; 13(6):e0198531. https://doi.org/10.1371/journal.pone.0198531 PMID: 29902192

27. Sachse F, Ahlers F, Stoll W, Rudack C. Neutrophil chemokines in epithelial inflammatory processes of human tonsils. Clin Exp Immunol. 2005; 140(2):293–300. https://doi.org/10.1111/j.1365-2249.2005.02773.x PMID: 15807854.

28. Gschwandtner M, Derler R, Midwood KS. More Than Just Attractive: How CCL2 Influences Myeloid Cell Behavior Beyond Chemotaxis. Frontiers in Immunology. 2019; 10. https://doi.org/10.3389/fimmu.2019.02759 PMID: 31921102

29. Zeng Z, Lan T, Wei Y, Wei X. CCL5/CCR5 axis in human diseases and related treatments. Genes Dis. 2022; 9(1):12–27. Epub 20210826. https://doi.org/10.1016/j.gendis.2021.08.004 PMID: 34514075.

30. Imai T, Baba M, Nishimura M, Kakizaki M, Takagi S, Yoshie O. The T Cell-directed CC Chemokine TARC Is a Highly Specific Biological Ligand for CC Chemokine Receptor 4*. Journal of Biological Chemistry. 1997; 272(23):15036–42. https://doi.org/10.1074/jbc.272.23.15036 PMID: 9169480

31. Matti C, D'Uonnolo G, Artinger M, Melgrati S, Salnikov A, Thelen S, et al. CCL20 is a novel ligand for the scavenging atypical chemokine receptor 4. Journal of Leukocyte Biology. 2020; 107(6):1137–54. https://doi.org/10.1002/JLB.2MA0420-295RRR PMID: 32533638

32. Mandal PK, Biswas S, Mandal G, Purohit S, Gupta A, Majumdar A, et al. CCL2 conditionally determines CCL22-dependent Th2-accumulation during TGF-β-induced breast cancer progression. Immunobiology. 2018; 223(2):151–61. https://doi.org/10.1016/j.imbio.2017.10.031 PMID: 29107385

33. Karin N, Razon H. Chemokines beyond chemo-attraction: CXCL10 and its significant role in cancer and autoimmunity. Cytokine. 2018; 109:24–8. https://doi.org/10.1016/j.cyto.2018.02.012 PMID: 29449068

34. Winer H, Rodrigues GOL, Hixon JA, Aiello FB, Hsu TC, Wachter BT, et al. IL-7: Comprehensive review. Cytokine. 2022; 160:156049. https://doi.org/10.1016/j.cyto.2022.156049 PMID: 36201890

35. Zhu J. T Helper Cell Differentiation, Heterogeneity, and Plasticity. Cold Spring Harb Perspect Biol. 2018; 10(10). Epub 20181001. https://doi.org/10.1101/cshperspect.a030338 PMID: 28847903.

36. Bonner K, Pease JE, Corrigan CJ, Clark P, Kay AB. CCL17/thymus and activation-regulated chemokine induces calcitonin gene–related peptide in human airway epithelial cells through CCR4. Journal of Allergy and Clinical Immunology. 2013; 132(4):942–50.e3. https://doi.org/10.1016/j.jaci.2013.04.015 PMID: 23731651

37. Walker JA, McKenzie ANJ. TH2 cell development and function. Nature Reviews Immunology. 2018; 18 (2):121–33. https://doi.org/10.1038/nri.2017.118 PMID: 29082915

38. Groom JR, Luster AD. CXCR3 in T cell function. Experimental Cell Research. 2011; 317(5):620–31. https://doi.org/10.1016/j.yexcr.2010.12.017 PMID: 21376175

39. Panopoulos AD, Watowich SS. Granulocyte colony-stimulating factor: molecular mechanisms of action during steady state and 'emergency' hematopoiesis. Cytokine. 2008; 42(3):277–88. Epub 20080408. https://doi.org/10.1016/j.cyto.2008.03.002 PMID: 18400509.

40. Conlon TM, John-Schuster G, Heide D, Pfister D, Lehmann M, Hu Y, et al. Inhibition of LTβR signalling activates WNT-induced regeneration in lung. Nature. 2020; 588(7836):151–6. https://doi.org/10.1038/s41586-020-2882-8 PMID: 33149305

41. Mikami Y, Matsuzaki H, Horie M, Noguchi S, Jo T, Narumoto O, et al. Lymphotoxin β receptor signaling induces IL-8 production in human bronchial epithelial cells. PLoS One. 2014; 9(12):e114791. Epub 20141211. https://doi.org/10.1371/journal.pone.0114791 PMID: 25501580.

42. Butt Y, Kurdowska A, Allen TC. Acute Lung Injury: A Clinical and Molecular Review. Arch Pathol Lab Med. 2016; 140(4):345–50. https://doi.org/10.5858/arpa.2015-0519-RA PMID: 27028393.

43. Gulati K, Gangele K, Agarwal N, Jamsandekar M, Kumar D, Poluri KM. Molecular cloning and biophysical characterization of CXCL3 chemokine. International Journal of Biological Macromolecules. 2018; 107:575–84. https://doi.org/10.1016/j.ijbiomac.2017.09.032 PMID: 28928065

44. Lopez-Castejon G, Brough D. Understanding the mechanism of IL-1β secretion. Cytokine & Growth Factor Reviews. 2011; 22(4):189–95. https://doi.org/10.1016/j.cytogfr.2011.10.001 PMID: 22019906

45. Holbrook J, Lara-Reyna S, Jarosz-Griffiths H, McDermott M. Tumour necrosis factor signalling in health and disease. F1000Res. 2019; 8. Epub 20190128. https://doi.org/10.12688/f1000research.17023.1 PMID: 30755793.

46. Foulon M, Robbe-Saule M, Manry J, Esnault L, Boucaud Y, Alcaïs A, et al. Mycolactone toxin induces an inflammatory response by targeting the IL-1β pathway: Mechanistic insight into Buruli ulcer pathophysiology. PLOS Pathogens. 2020; 16(12):e1009107. https://doi.org/10.1371/journal.ppat.1009107 PMID: 33338061

47. Osawa R, Williams KL, Singh N. The inflammasome regulatory pathway and infections: Role in pathophysiology and clinical implications. Journal of Infection. 2011; 62(2):119–29. https://doi.org/10.1016/j.jinf.2010.10.002 PMID: 20950647

48. Grötzinger J, Lorenzen I, Düsterhöft S. Molecular insights into the multilayered regulation of ADAM17: The role of the extracellular region. Biochimica et Biophysica Acta (BBA)—Molecular Cell Research. 2017; 1864(11, Part B):2088–95. https://doi.org/10.1016/j.bbamcr.2017.05.024 PMID: 28571693

49. McClurg UL, Danjo K, King HO, Scott GB, Robinson PA, Crabtree JE. Epithelial cell ADAM17 activation by Helicobacter pylori: role of ADAM17 C-terminus and Threonine-735 phosphorylation. Microbes and Infection. 2015; 17(3):205–14. https://doi.org/10.1016/j.micinf.2014.11.011 PMID: 25499189

50. Hausmann A, Felmy B, Kunz L, Kroon S, Berthold DL, Ganz G, et al. Intercrypt sentinel macrophages tune antibacterial NF-κB responses in gut epithelial cells via TNF. Journal of Experimental Medicine. 2021; 218(11). https://doi.org/10.1084/jem.20210862 PMID: 34529751

51. Shiratori T, Imaizumi T, Hirono K, Kawaguchi S, Matsumiya T, Seya K, et al. ISG56 is involved in CXCL10 expression induced by TLR3 signaling in BEAS-2B bronchial epithelial cells. Experimental Lung Research. 2020; 46(6):195–202. https://doi.org/10.1080/01902148.2020.1760965 PMID: 32363951

52. Berin MC, Dwinell MB, Eckmann L, Kagnoff MF. Production of MDC/CCL22 by human intestinal epithelial cells. American Journal of Physiology-Gastrointestinal and Liver Physiology. 2001; 280(6):G1217–G26. https://doi.org/10.1152/ajpgi.2001.280.6.G1217 PMID: 11352815.

53. Chen Y-H, Zhou B-Y, Wu X-J, Xu J-F, Zhang JA, Chen Y-H, et al. CCL22 and IL-37 inhibit the proliferation and epithelial-mesenchymal transition process of NSCLC A549 cells Corrigendum in /10.3892/

or.2020.7903. Oncol Rep. 2016; 36(4):2017–24. https://doi.org/10.3892/or.2016.4995 PMID: 27499437

54. He M, Song G, Yu Y, Jin Q, Bian Z. LPS-miR-34a-CCL22 axis contributes to regulatory T cell recruitment in periapical lesions. Biochemical and Biophysical Research Communications. 2015; 460(3):733–40. https://doi.org/10.1016/j.bbrc.2015.03.098 PMID: 25817785

55. Robison HM, Escalante P, Valera E, Erskine CL, Auvil L, Sasieta HC, et al. Precision immunoprofiling to reveal diagnostic signatures for latent tuberculosis infection and reactivation risk stratification. Integrative Biology. 2019; 11(1):16–25. https://doi.org/10.1093/intbio/zyz001 PMID: 30722034

56. Robison HM, Chapman CA, Zhou H, Erskine CL, Theel E, Peikert T, et al. Risk assessment of latent tuberculosis infection through a multiplexed cytokine biosensor assay and machine learning feature selection. Scientific Reports. 2021; 11(1):20544. https://doi.org/10.1038/s41598-021-99754-3 PMID: 34654869